Multiplexed holographic transmission gratings recorded in holographic polymer-dispersed liquid crystals: static and dynamic studies

Sébastien Massenot, Jean-Luc Kaiser, Maria Camacho Perez, Raymond Chevallier, and Jean-Louis de Bougrenet de la Tocnaye

The optimization of the experimental parameters of two multiplexed holographic transmission gratings recorded in holographic polymer-dispersed liquid crystals is investigated. Two methods are used to record the holograms: simultaneous and sequential multiplexing. These two processes are optimized to produce two multiplexed Bragg gratings that have the same and the highest possible diffraction efficiencies in the first order. The two methods show similar results when suitable recording parameters are used. The parameters of the recorded gratings (mainly the refractive-index modulation) are retrieved by use of an extension of the rigorous coupled-wave theory to multiplexed gratings. Finally, the response of the holograms to an electric field is studied. We demonstrate few coupling effects between the behavior of both gratings, and we expect a possibility of switching from one grating to the other.

1. Introduction

Holographic polymer-dispersed liquid crystals (H-PDLCs) have already shown a promising future, especially in optical information processing, color reflective displays,[1] and telecommunications.[2] This holographic material has the combined advantages of photopolymers (self-processing material, easy development robustness) and the properties of liquid crystals, which provide a switchable behavior with larger electro-optic effects under low voltage. Such holograms are composed of a succession of polymer-rich planes and liquid-crystal-rich planes. They are obtained through a holographic process: An interference pattern induces photopolymerization in the constructive interference zones, and the monomers diffuse from low exposed zones to strongly exposed zones. At the same time, the liquid crystal migrates in the opposite direction and forms droplets, as shown in Fig. 1.

By choosing the materials judiciously such that the refractive index of the polymer is equal to the ordinary index of the liquid crystal, it is possible to erase the hologram totally by applying an electric field. Electrically switchable components have already been fabricated with this technique (Bragg gratings[3] and switchable lenses,[4] for example).

To obtain more-complex functions, one generally stacks several different holograms. To avoid the need for stacking of components, it would be useful to investigate whether several holograms can be recorded in the same H-PDLC cell, enabling several functions to be performed simultaneously and cost effectively.

In contrast to recording several holograms in conventional holographic materials such as dichromated gelatin, doing so in self-processing materials (H-PDLCs, photopolymers) requires some precautions. Once the hologram is recorded in this material, monomers consumed during the recording process are not reusable and will disturb subsequent diffusion of the remaining monomers. The material undergoes a kind of passivation.

If we want to multiplex holograms in H-PDLCs it is necessary to know which parameters are critical and should be controlled to obtain good-quality holograms. In this paper we propose to study the forma-

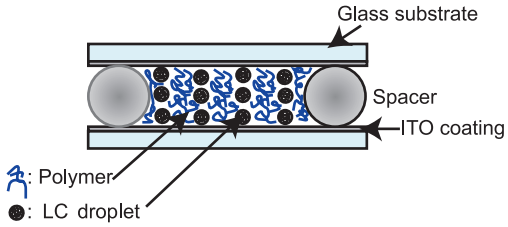

Fig. 1. (Color online) H-PDLC structure after recording. ITO, indium tin oxide; LC, liquid crystal.

tion of two different period holographic transmission Bragg gratings (which are the simplest possible holograms) in a H-PDLC (see Fig. 2). The holograms are characterized from static and dynamic points of view.

With such structures containing two collinear periodicities we have to face several problems during recording. Recording parameters have to be adjusted such that the two gratings have the same and the highest possible diffraction efficiency in the first order. To do this, we studied two recording techniques: simultaneous multiplexing, in which the two gratings grow together, and sequential multiplexing, in which the gratings are recorded successively. The advantages and disadvantages of these two methods are discussed below.

As a consequence, such structures present different concentrations and sizes of liquid-crystal droplets. Some of them are smaller than others and undergo greater constraints when an electric field is applied. The electro-optic behavior of the component changes as a result.

After an introduction to the multiplexing of holograms in photopolymerizable materials, we describe the theoretical tool used to calculate multiplexed gratings. This tool helps us to retrieve the refractive-index modulations of the two gratings, which is an interesting result of characterizing such materials. These values are the critical parameters in a static study of the hologram. Then the optimization of the recording parameters for the two experimental setups (simultaneous and sequential multiplexing) are presented. We conclude with a presentation of the dynamic characterization of such holograms under an applied electric field.

2. Hologram Multiplexing in H-PDLCs

One component of the formation of H-PDLCs is photopolymerization and monomer transport. From this point of view, H-PDLCs behave as photopolymers.

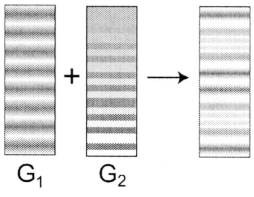

Fig. 2. Multiplexing of two transmission Bragg gratings.

Recording techniques used for these materials can be directly applied to H-PDLCs.

A. State of the Art

Previous research has demonstrated the recording of two diffraction gratings in photopolymers, but in those cases the gratings were slanted and had the same periods[5,6] (the fringes of the two gratings were symmetrically slanted with regard to the normal of the surface). In this configuration the formation kinetics of the two gratings are assumed to be the same. Several slanted fringe transmission gratings with an optimization of the recording procedure have been obtained in photopolymers with similar diffraction efficiencies for each grating.[7] In our case, the two gratings have different periods, which means that each has its own formation kinetic. During recording, strong competition will occur between the formation of the two gratings. Studies of crossed gratings recorded in photopolymers have been obtained[8] that show the spatial dependence of the photopolymerization and the monomer transport. The diffusion associated with the second grating is weakly perturbed by the first (monomers diffuse in orthogonal directions).

With respect to H-PDLCs, several multiplexing studies have been made[9,10] that were oriented more toward reflective displays. The combination of transmission and reflection gratings with photonic crystal structures has also been studied.[11,12]

Here we study in detail the formation kinetics of two transmission gratings (with symmetrical fringes) to see which critical parameters are involved and the way in which they could be useful for improving the recording of more-complex structures with a larger multiplex. We also wish to optimize the recording process to get two gratings with the same and maximum diffraction efficiencies.

B. Physical Aspects of Recording Multiplexed Holograms

The diffusion equation for the monomer concentration with an exposure pattern containing two systems of parallel interference fringes of periods Λ_1 and Λ_2 is of the form (according to Ref. 13) of

$$\frac{\partial \phi(x,\,t)}{\partial t} = \frac{\partial}{\partial x}\left[D(x,\,t)\frac{\partial \phi(x,\,t)}{\partial x}\right] - \left\{F_0^{(1)}\left[1+\cos\left(\frac{2\pi}{\Lambda_1}x\right)\right]^{1/2} + F_0^{(2)}\left[1+\cos\left(\frac{2\pi}{\Lambda_2}x\right)\right]^{1/2}\right\}\phi(x,\,t), \quad (1)$$

where $\phi(x, t)$ is the monomer concentration, $D(x, t)$ is the diffusion coefficient, and $F_0^{(1)}$ and $F_0^{(2)}$ are the polymerization rates associated with the two gratings ($F_0 = \kappa\sqrt{I_0}$, where κ is the polymerization rate coefficient and I_0 is the irradiance associated with the recording beams).

Such an equation is quite difficult to solve. The form of the solution for monomers is a two-

dimensional Fourier expansion that takes into account the contributions of the two periodicities.

In addition, several specific phenomena that occur in H-PDLCs (anisotropic phase separation, incoherent scattering, incomplete phase separation), as well as the difficulty in learning precisely the value of some material constitutive parameters, mean that the study of such recordings has to be made experimentally. One can perform the optimization by studying in real time the formation of the hologram.[14] As was mentioned above, two periodic systems are formed in the material. In our case the objective is to obtain gratings that have the highest and balanced diffraction efficiencies under Bragg incidence.

3. Modeling of Multiplexed Diffraction Gratings

Multiplexed holographic gratings can be modeled with the rigorous coupled-wave theory for isotropic media.[15] The original method has been extended to gratings with two periodicities that can be oriented independently of each other. This technique allows us to calculate multiplexed gratings (the grating vectors are parallel) as crossed gratings (grating vectors are perpendicular). Implementations of the extension of rigorous coupled-wave theory to two-dimensional gratings can be found in Refs. 16 and 17.

A. Improvements

Recent improvements in the rigorous coupled-wave theory were used; they include notably the scattering matrix algorithm,[18] which lends an unconditional stability to the method, as well as factorization rules for Fourier series of the product of two periodic functions, and they allow us to work with only continuous components of electric field $\mathbf{E}$.[19,20]

B. Simulations of Multiplexed Gratings

Below, we show some examples of multiplexed holographic gratings and study their differences from two single gratings. In the first case (Fig. 3), we consider two gratings whose periods are similar ($\Lambda_1 = 1.3$ μm and $\Lambda_2 = 2.1$ μm) so there is an overlap between the responses of the two gratings. The thickness of the gratings is fixed at 18 μm (this value corresponds to the size of the spacers that we used to obtain the H-PDLC cells), and the gratings have the same refractive-index modulation, $\Delta n = 0.015$.

In this configuration, coupling effects occur between the two gratings, and their respective diffraction efficiencies decrease.

When the Bragg angles are quite different (Fig. 4), the perturbation of one grating by the other becomes less significant. Simulation parameters are the same as described above, except that the period of the first grating is 0.7 μm.

To begin with, we choose gratings with widely different periods to prevent coupling effects between them and so obtain the maximum diffraction efficiency.

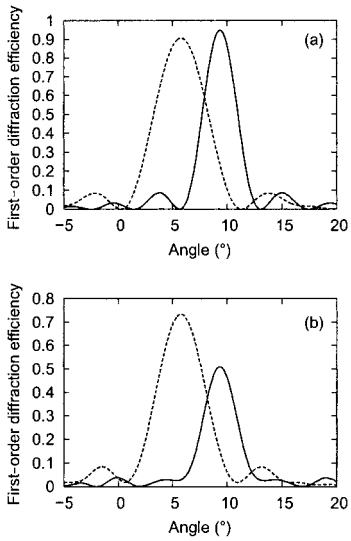

Fig. 3. Comparison of the angular selectivities of holographic transmission of similar period diffraction gratings: (a) separate, (b) multiplexed.

4. Experimental Setup

A. Recording

The recording setup used is illustrated in Fig. 5. Two pairs of mutually incoherent beams coming from an Ar^+ laser at 514.5 nm are generated (labeled A1 and A2 and B1 and B2 in Fig. 5) to prevent the formation of parasite gratings. Shutters and neutral-density filters are placed in the different optical paths to adjust the recording parameters (exposure time and irradiance).

The optical path difference between the two paths corresponding to the two gratings is not high enough with regard to the coherence length of the Ar^+ laser. A half-wave plate has been added to the path corre-

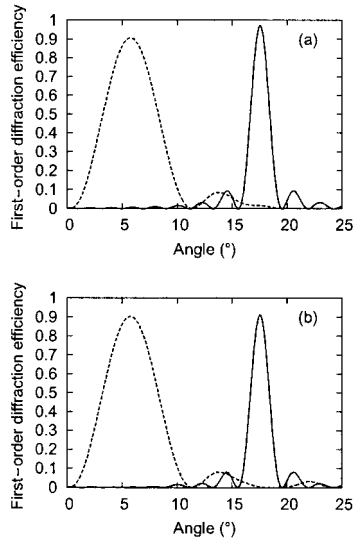

Fig. 4. Comparison of the angular selectivities of holographic transmission diffraction gratings with widely differing periods: (a) separate, (b) multiplexed.

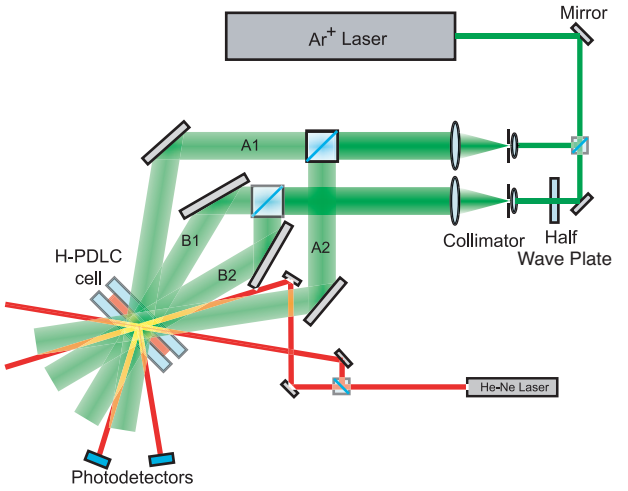

Fig. 5. (Color online) Experimental setup for recording.

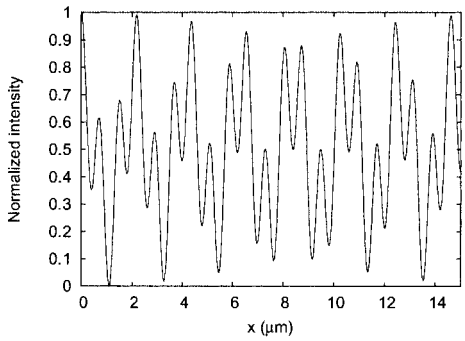

Fig. 6. Interference pattern for simultaneous multiplexing (which corresponds to beating between two sinusoidal patterns).

sponding to one grating to work with beams that have crossed polarizations. This half-wave plate is added to the path corresponding to the grating that has the longest period, a loss of contrast will occur because the polarization of the beams will undergo a reorientation after the reflection on the mirrors (the two polarizations will not be parallel).

In this way, the presence of unwanted gratings is prevented. The half-wave plate is removed when the gratings are recorded sequentially.

In addition, two beams from a He–Ne laser at 632.8 nm are used to illuminate the H-PDLC cell at Bragg incidence to visualize in real time the formation of each of the two gratings. In this way we are able to quantify the different rates of formation for the different gratings.

B. Parameters of the H-PDLC Mixture

The H-PDLC homogeneous mixture is made from a principal monomer, Ebecryl 1290 (30%); two comonomers, vinyl neononanoate (15%), and hexafluoropropyl acrylate (15%); a liquid crystal, BL036 (30%); and a photoinitiator solution (10%) composed of the colorant Rose Bengal (3%), the coinitiator *N*-phenylglycine (7%), and two reactive diluents, 1-vinyl-2-pyrrolidinone (45%) and trimethylolpropane tris(3-mercaptoproprionate) (45%).

We then obtain H-PDLC cells by sandwiching a polymer mixture between two glass substrates covered with conductive indium tin oxide layers. First spacers of 18 μm were sprayed on the substrates to guarantee the thickness of the cell (Fig. 1).

After exposure to interference patterns, the cells underwent an UV postexposure to consume the remaining monomers and the Rose Bengal colorant.

5. Simultaneous Recording

A. Introduction

In this configuration, the monomer diffusion associated with a grating will be strongly disturbed by the formation of the second grating. In addition, locally the contrast of the fringes of the interference pattern is not optimal because there are zones where the exposure energy has an intermediate level. For example, if we record two gratings of periods $\Lambda_1 = 0.73$ μm and $\Lambda_2 = 2.1$ μm and assume that all the beams used for the recording have the same power and that the contrast of the fringes generated by each beam pair is maximum, the interference pattern looks like the curve shown in Fig. 6.

We can see that the way in which the hologram is formed differs according to the location and that the formation of the liquid-crystal droplets is affected such that the droplets have different sizes.

For the two gratings the competition between the two phenomena that participate in the recording process (monomer diffusion and polymerization) is not the same, which produces an imbalance in the formation of the two gratings (one grating will grow faster than the other). To have similar diffraction efficiencies it becomes necessary to adjust the power of the recording beams to limit the dominance of the faster-growing grating.

B. Recording of Separate Gratings

We made some preliminary recordings of separate gratings to see how the two gratings form independently of each other and whether one grows faster than the other. We represent in Figs. 7(a) and 7(b) the time evolution of the first-order diffraction efficiencies of gratings of periods 0.73 and 2.1 μm, respectively.

Note that for similar exposure energies the 2.1 μm grating grows faster than the 0.73 μm grating. We must therefore slow down the formation kinetic of this grating by exposing the grating to a lower energy to make both gratings grow at the same speed.

C. Optimization of the Recording Parameters

An example of optimization of the recording parameters in simultaneous multiplexing is shown in Fig. 8. The irradiance relative to the 0.73 μm grating was kept constant at a value of 51.5 mW/cm^2, and we varied the irradiance associated with the 2.1 μm grating.

As we can see, the irradiance of the two gratings needs to be strongly imbalanced (nearly a ratio 1:2) if

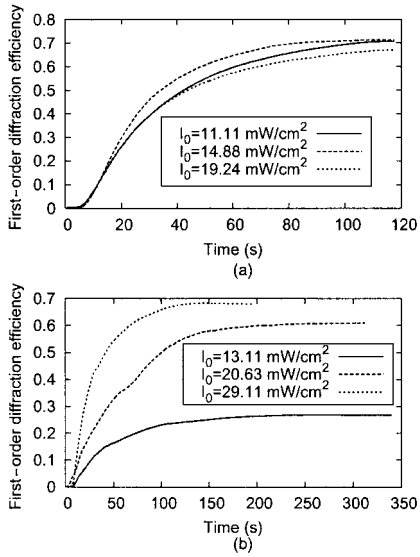

Fig. 7. Evolution of the first diffracted orders for three exposure energies I_0 for gratings of periods (a) 2.1 μm and (b) 0.73 μm.

we want the two gratings to grow at the same speed and give maximum diffraction efficiencies. The holographic material is quite sensitive to variations in exposure energy; one grating can dominate the other quickly, disturb it, and even prevent its formation. In addition, we can remark that for each recording a change in the formation rate occurs near 50 s. We assume that this is so because there are several monomers in the material that are not consumed at the same rate.

We show in Fig. 9 a recording result in which the two gratings are quite well balanced: The exposure energies are 16.66 mW/cm^2 for the 2.1 μm grating and 36.38 mW/cm^2 for the 0.73 μm grating.

The reason that we cannot reach diffraction efficiencies close to 100% is that the maximum refractive-index modulation obtainable with our material is too small. If we denote by $\Delta n_{\max}$ the highest refractive-index modulation that can be obtained with our material and record N gratings, $\Delta n_{\max}$ will be distributed between these N gratings such that $\sum_{i=1}^{N} \Delta n_i = \Delta n_{\max}$.[5]

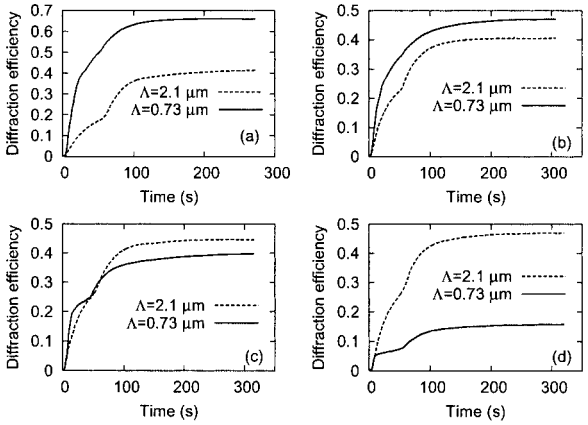

Fig. 8. Optimization of the recording parameters for simultaneous multiplexing. The variable parameter is the irradiance used for the 2.1 μm grating: (a) I_0 = 17.1 mW/cm^2, (b) I_0 = 24.5 mW/cm^2, (c) I_0 = 25.7 mW/cm^2, (d) I_0 = 26.8 mW/cm^2.

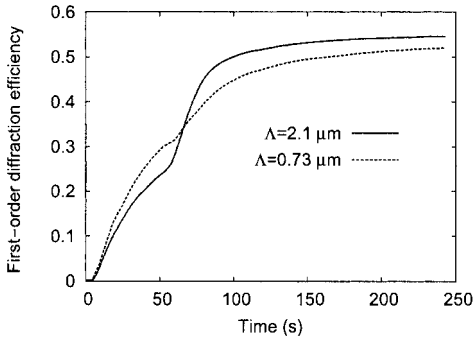

Fig. 9. Balanced multiplexed gratings obtained with the simultaneous recording setup.

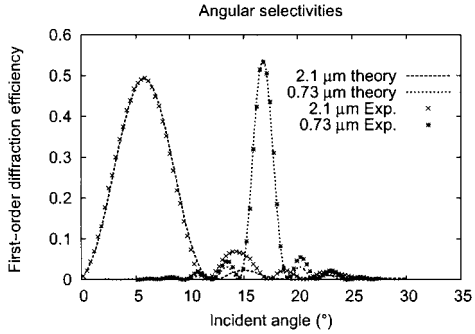

Fig. 10. Angular characterization of two multiplexed gratings: comparison of experimental results (dotted curves) and theoretical prediction (continuous curves).

Such a hologram was angularly characterized with a TE-polarized He–Ne laser at 632.8 nm. Two-dimensional rigorous coupled-wave theory allows us to retrieve the refractive-index modulation associated with each grating by adjusting simulation parameters to fit experimental results. The results are shown in Fig. 10.

We obtained the following refractive-index modulations: $\Delta n_{\Lambda=2.1\ \mu m} = 0.0088$ and $\Delta n_{\Lambda=0.73\ \mu m} = 0.0091$, so we have $\Delta n_{\max}$ at least equal to 0.0179 (similar values are reported in Ref. 14). These values, which are provided by the theory, are for gratings made from isotropic media; as this is not true in the case that we are studying, we obtain an effective index modulation for the TE polarization.

6. Sequential Recording

A. Introduction

From the monomer diffusion point of view, the sequential multiplexing provides the highest energy gradient, as the fringe contrast is maximum for each recording. The recording of the first grating, however, can strongly disturb the formation of the second grat-

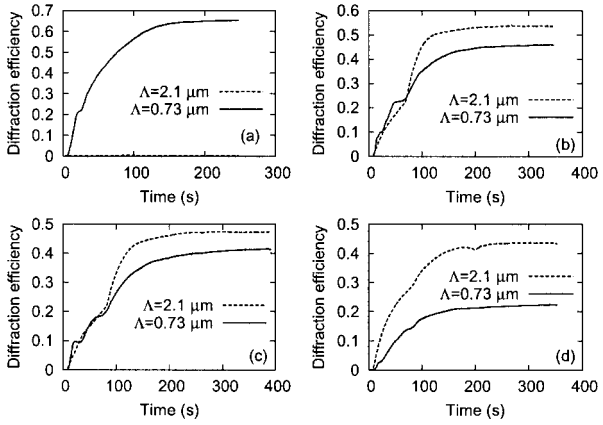

Fig. 11. Time evolution of the first-order diffraction efficiency of two sequentially multiplexed transmission gratings with different exposure times for the first grating: (a) 3 s, (b) 4.3 s, (c) 4.5 s, (d) 5 s.

ing. In fact, if the first one is recorded and fixed in the material, it will be difficult for the remaining monomers to diffuse correctly during the second exposure. As previously, the choice of the exposure energies associated with each grating will be essential, but, consequently, the exposure time of the first grating must be determined. It seems straightforward to record the longer-period grating first to allow the formation of the second one (the diffusion of the monomers will be easier).

B. Optimization of the Recording Parameters

We maintain the exposure energies associated with the two gratings constant [16.13 mW/cm^2 (2.1 μm) and 32 mW/cm^2 (0.73 μm)] and vary only the exposure time of the first grating. Recording results are shown in Fig. 11. Figures 11(a), 11(b), 11(c), and 11(d), correspond to first grating exposure times of 3, 4.3, 4.5, and 5 s, respectively, for the 2.1 μm grating.

We remark that the optimum exposure time for the first grating (in our experimental conditions) is quite short (~4.3 s) and that the gratings continue to form during the second exposure.

The exposure time of the first grating seems to be a critical parameter. In our case, 3 s is not enough to start the formation of the grating and 5 s is too long if we want to obtain balanced gratings.

7. Electro-Optical Properties

A. When the Angular Responses Do Not Overlap

We dynamically characterized the previously recorded holograms by studying their response to an applied voltage (a square wave at 1 kHz) at Bragg incidence for each grating. To simplify the comparison, in Fig. 12 we plot normalized diffraction efficiencies versus the applied electric field.

We can remark that the 2.1 μm grating switches faster than the other and that the electric fields are less than 8 V/μm. This is so because the droplets involved in this grating are larger than the droplets associated with the grating of 0.73 μm, so they switch

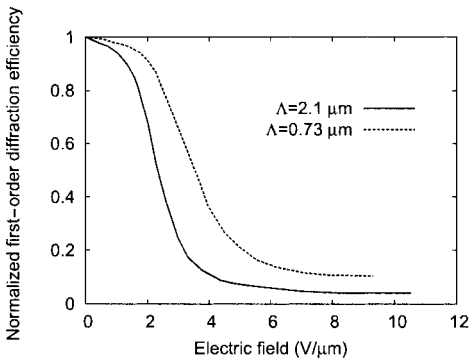

Fig. 12. Normalized diffraction efficiency in the first order for the two gratings as a function of the applied electric field.

at lower voltages. It even seems possible to erase one grating by keeping the other at a high diffraction efficiency. A disadvantage is that to observe such effects we need two incident beams.

B. When the Angular Responses Overlap

We saw in Section 3 [Fig. 3(b)] that, when the angular responses of the gratings overlap, coupling effects occur between the diffraction efficiencies of the two gratings. If we work not at Bragg incidence but at an intermediary angle where the curves of diffraction efficiencies are crossing [Fig. 3(b)], we can expect a modification of this coupling by applying an electric field and even switch from one grating to the other. In our configuration, we have a loss in diffraction efficiency that is due to the fact that we are working with one beam with an incidence between the Bragg angles of the two gratings. The grating periods that we chose were $\Lambda_1 = 1.3$ μm and $\Lambda_2 = 2.1$ μm.

From Fig. 13 we can see few coupling effects between the two gratings, as if the energy of one were transferred to the other. This effect is not efficient; it is possible to improve it by having higher refractive-index modulations for the two gratings. For this purpose, the phase separation during recording has to be improved. An advantage is that the switching effects occur for values of the electric field smaller than

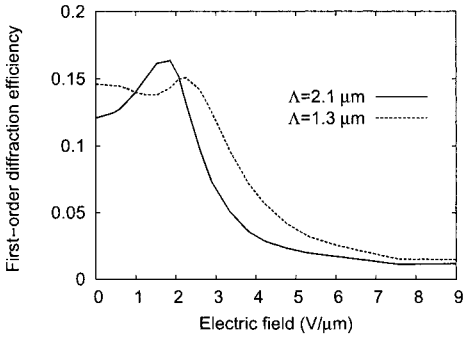

Fig. 13. Diffraction efficiency in the first order for the two gratings as a function of the applied electric field when the angle of incidence is between the two Bragg angles.

3 V/μm. Variable beam deflectors and spectral band selectors could be derived from this effect.

As in Subsection 6.A, beyond a certain voltage the two gratings begin to be erased, and the grating that has the shorter period switches more slowly than the other period.

8. Conclusions

We have studied static and dynamic behavior of the multiplexing of two transmission gratings in H-PDLCs. We have described how to optimize two experimental setups to grow both gratings at the same speed during the recording process. We obtained similar results for the two multiplexing methods (simultaneous and sequential), but each of them requires specific recording parameters.

In the case of simultaneous multiplexing the critical parameters are the irradiances associated with the recording beam. Exposure energies have to be adjusted to produce a balanced competition between the diffusion of the monomers and the photopolymerization for the two gratings. For the sequential recording the exposure time of the first grating is critical because, if this time is too long, the first grating will prevent correct diffusion of monomers for the second grating. For the static characterization we retrieved an estimation of the refractive-index modulations of the two gratings for TE polarization by using rigorous coupled-wave theory. We checked that the global refractive-index modulation that can be obtainable is shared between the different recorded gratings. This effect strongly limits the number of holograms that can be recorded in the material. We can estimate this number as ten; this material is not appropriate for recording hundreds of holograms.

We have demonstrated the existence of some coupling effects between two gratings when an electric field is applied. It seems possible to amplify these effects with more-elaborate work on the H-PDLC material (by having a better phase separation to reach higher refractive-index modulations). With consequent coupling, we suspect that it will be possible to switch electrically from one grating to the other. An amplification of this switching effect could lead to several interesting applications: selection of a spectral band and optical switches, for example.

To improve the diffraction efficiencies and to reach values close to 100% we can either increase the thickness of the cells or work on the H-PDLC material to reach a higher global refractive-index modulation $\Delta n_{\max}$. However, the thickness cannot be increased indefinitely because of the kinetics of the curing process. The second application could be achieved with better phase separation between polymer and liquid crystals and control of the orientation of the director of the liquid droplets (to have a higher index difference between liquid droplets and the polymer).

With reference to the recording process, a solution to amplifying the switching effect could be to change the configuration of one of the gratings. The first grating would still be transmissive, with fringes orthogonal to the substrates, whereas the second grating would have slanted fringes to make both gratings work at Bragg incidence instead of at an intermediary incident angle. Both will have higher diffraction efficiencies, but it will be more complicated to achieve the recording setup because of shrinkage effects that occur with photopolymerizable materials. One has to study this effect precisely to obtain a second grating with the same Bragg angle as the first grating. Another suggestion could be the use of digital holography to generate the multiplex structure and to replicate this structure in H-PDLCs.

References

1. A. K. Fontecchio, C. C. Bowley, S. M. Chmura, L. Li, S. Faris, and G. P. Crawford, "Multiplexed holographic polymer dispersed liquid crystals," J. Opt. Technol. **68,** 652–656 (2001).
2. J. L. Kaiser, G. P. Crawford, R. Chevallier, and J. L. de Bougrenet de la Tocnaye, "Chirped switchable reflection grating in holographic PDLC for wavelength management and processing in optical communication systems," Appl. Opt. **43,** 5996–6000 (2004).
3. T. J. Bunning, L. V. Natarajan, V. P. Tondiglia, and R. L. Sutherland, "Holographic polymer-dispersed liquid crystals (H-PDLCs)," Annu. Rev. Mater. Sci. **30,** 83–115 (2000).
4. H. Ren and S. Wu, "Inhomogeneous nanoscale polymer-dispersed liquid crystals with gradient refractive index," Appl. Phys. Lett. **81,** 3537–3539 (2002).
5. S. Piazzolla and B. K. Jenkins, "Dynamics during holographic exposure in photopolymers for single and multiplexed gratings," J. Mod. Opt. **46,** 2079–2110 (1999).
6. X. Han, G. Kim, and R. T. Chen, "Accurate diffraction efficiency control for multiplexed volume holographic gratings," Opt. Eng. **41,** 2799–2802 (2002).
7. C. Carré, P. Saint-Georges, L. Bigué, and F. Christnacher, "Advanced photopolymerizable material for creation of particular diffractive optical elements," in *Holography, Diffractive Optics, and Applications*, D. Hsu, J. Chen, and Y. Sheng, eds., Proc. SPIE **4924,** 322–333 (2002).
8. R. K. Kostuk, "Dynamic hologram recording in Dupont photopolymers," Appl. Opt. **38,** 1357–1363 (1999).
9. C. C. Bowley, A. K. Fontecchio, and G. P. Crawford, "Multiple gratings simultaneously formed in holographic polymer-dispersed liquid-crystal displays," Appl. Phys. Lett. **76,** 523–525 (2000).
10. M. E. Sousa, J. Qi, M. J. Escuti, and G. P. Crawford, "Mesoscales lattices and temporal multiplexing in liquid crystal/polymer dispersions," in *Liquid Crystals VII*, I.-C. Khoo, ed., Proc. SPIE **5213,** 130–138 (2003).
11. M. J. Escuti, J. Qi, and G. P. Crawford, "Tunable face-centered-cubic photonic crystal formed in holographic polymer dispersed liquid crystals," Opt. Lett. **28,** 522–524 (2003).
12. R. L. Sutherland, V. P. Tondiglia, L. V. Natajaran, S. Chandra, D. Tomlin, and T. J. Bunning, "Switchable orthorhombic F photonic crystals formed by holographic polymerisation-induced phase separation of liquid crystals," Opt. Express **10,** 1074–1082 (2002).
13. G. Zhao and P. Mouroulis, "Diffusion model of hologram formation in dry photopolymerisable materials," J. Mod. Opt. **41,** 1929–1939 (1994).
14. S. Massenot, J. L. Kaiser, R. Chevallier, and Y. Renotte, "Study of the dynamic formation of transmission gratings recorded in photopolymers and holographic polymer-dispersed liquid crystals," Appl. Opt. **43,** 5489–5497 (2004).
15. M. G. Moharam, E. B. Grann, D. A. Pommet, and T. K. Gaylord, "Formulation for stable and efficient implementation of the rigorous coupled-wave analysis of binary gratings," J. Opt. Soc. Am. A **12,** 1068–1076 (1995).

16. M. Nevière and E. Popov, *Light Propagation in Periodic Media, Differential Theory and Design* (Marcel Dekker, 2003).
17. R. Bräuer and O. Bryngdahl, "Electromagnetic diffraction analysis of two-dimensional gratings," Opt. Commun. **100,** 1–5 (1993).
18. L. Li, "Formulation and comparison of two recursive matrix algorithms for modelling layered diffraction gratings," J. Opt. Soc. Am. A **13,** 1024–1035 (1996).
19. P. Lalanne and G. M. Morris, "Highly improved convergence of the coupled-wave method for TM polarization," J. Opt. Soc. Am. A **13,** 779–784 (1996).
20. L. Li, "Use of Fourier series in the analysis of discontinuous periodic structures," J. Opt. Soc. Am. A **13,** 1870–1876 (1996).